

A FOUR-METER LONG SUPERCONDUCTING MAGNETIC
FLUX EXCLUSION TUBE
FOR PARTICLE PHYSICS EXPERIMENTS*

F. Martin, S. J. St. Lorant, W. T. Toner†
Stanford Linear Accelerator Center
Stanford University, Stanford, California 94305

Abstract

The design and construction of a field-free channel through the transverse central magnetic field of a 54-inch aperture magnet is described. This flux-free path is an essential part of an experiment at the Stanford Linear Accelerator Center to measure the electron production of neutral rho mesons. The flux exclusion tube itself is made of Nb₃Sn tape bonded with lead-tin solder to form a rigid tube of laminated superconducting material, approximately four meters long and from 6 to 25 mm in diameter. The transverse magnetic field shielded exceeds 1.5 T. The performance of the tube and its associated cryostat is discussed.

*Work supported by the U. S. Atomic Energy Commission.

†Now at Rutherford High Energy Laboratory, Chilton, Didcot, Berkshire, England.

1. Introduction

In this paper, we describe the design and construction of a superconducting flux exclusion tube 4 meters long and 1.3 cm average inside diameter, which is being used to create a field-free path through a transverse magnetic field of 1.5 tesla in an experiment at the Stanford Linear Accelerator Center. To the best of our knowledge, this is the first application of the flux exclusion properties of superconductors on such a large scale, and at these fields.

The experiment¹ is shown in Fig. 1. A 20-GeV/c electron beam containing 2×10^4 electrons per 1.4- μ sec pulse is incident on a liquid hydrogen target. In the reactions of interest, high-energy particles are produced at angles in excess of 30 mrad to the direction of the incident beam. These particles pass through an analyzing magnet with a peak field of 1.5 T and are detected in large area spark chambers and shower counters. Many photons, low-energy electrons and positrons are also produced in the target at very small angles to the beam, typically at angles of $\sim 2.5 \times 10^{-5}$ radians. The analyzing magnet would spread the charged particles out and create a severe background problem in the detection system, were it not for the superconducting flux exclusion tube through which they and the beam can pass without deflection.

The importance of creating a reduced-field path through the analyzing magnet was suggested to us by K. Heinloth,² the use of a superconductor to effect this by J. C. Pratt.³ In the course of our work, we learned that similar superconducting shields were being developed at CERN by Firth, Krempasky and Schmeissner,⁴ using many layers of copper-clad niobium-tin ribbon. The technique which we finally adopted is an extension of their method with the important difference that the individual layers of Cu-Nb₃Sn tape are bonded together with a lead-tin solder to form a rigid tube of laminated superconducting material.

In Section 2, we briefly discuss the basic theory of flux exclusion. Section 3 reviews some early development work, while Sections 4 and 5 are concerned with the results obtained with test samples of various designs. Section 6 describes the construction of the 4-meter tube and cryostat, and the performance is discussed in Section 7.

2. Some Remarks on Field Screening

When a magnetic field is applied to a hard superconductor below its transition temperature, a certain amount of the field will penetrate into the surface of the superconductor where it will induce screening supercurrents which will tend to keep the interior of the superconductor practically free from the magnetic field. Now, it is the basic premise of the theory of magnetization of hard superconductors⁵ that there exists a limiting macroscopic supercurrent density $J_c(B)$ which the superconductor can carry, determined uniquely by the local magnetic induction B . Thus, by Ampère's law, as the field is increased, the induced currents will spread into the interior of the superconductor. Up to the lower critical field, H_{c1} , the field is totally excluded by the surface currents. As soon as H_{c1} is exceeded, the flux begins to penetrate and superconducting regions immediately below the surface assume the mixed state. The rate of decrease of field with penetration depth is then evidently given by

$$\frac{dH}{dr} = -J_c \quad (1)$$

while the local value of the critical current density J_c is related to the induction B by the relation⁶

$$\alpha = J_c (B + B_0) \quad (2)$$

where both α and B_0 are constants of the material.

If α is evaluated at the operating temperature for the superconducting tape used in the present work, and if J_c is taken to be the average overall current density in the material, we find that $B_o = -.32$ T and $\alpha = 4.15 \times 10^{10}$ tesla amperes m⁻².

Combining Eq. (1) and (2) with $B = \mu_o H$, we obtain

$$\frac{dB}{dr} = - \frac{\mu_o \alpha}{B + B_o} \quad (3)$$

The solution of this expression is governed by the boundary conditions on the outside surface of the superconductor and the corresponding conditions in the interior where the field is just zero. If the external applied field is B_ϵ / μ_o , then at a point just outside the surface

$$B = \frac{B_\epsilon \sin \theta}{1 - n} \quad (4)$$

In the equatorial plane, this reaches the maximum value of the flux density

$$B_{\max} = 2 B_\epsilon$$

provided that the demagnetizing coefficient n is taken as $1/2$. The thickness of superconductor, ω , just sufficient to reduce the external field to zero is thus

$$\omega = \frac{B^2 + 2 B_o B}{2 \mu_o \alpha}$$

or

$$\omega_{\text{eq}} = \frac{2}{\mu_o \alpha} \left(B_\epsilon^2 + B_o B_\epsilon \right) \quad (5)$$

in the equatorial plane. To achieve complete shielding of an external field of 1.5 T, the superconductor should therefore be at least 90 μm thick.

For our long, hollow, cylindrical shell of constant thickness ω , placed in a uniform transverse field B_ϵ , the current distribution can be determined from

the boundary value solution, in terms of cylindrical harmonics, of the magnetic vector potential. It has the form

$$J_z = \frac{f(r) B_\epsilon \sin \theta}{\mu_o \omega (1 - n)} \quad (6)$$

where θ is the angle between the normal and the direction of the applied field. For a diamagnetic cylinder, $f(r) \cong 1$, and the maximum current density in a 1-mm thick shell in a field of 1.5 T is $2.4 \times 10^9 \text{ A m}^{-2}$. Also, the net induction at the exterior surface of the shell will be zero at $\theta = 0$, while it will be $2 B_\epsilon$ at $\theta = \pi/2, 3\pi/2$.

The interaction of the supercurrents and the applied field results in a static inward radial pressure on the cylinder, given by

$$p = \frac{2 B_\epsilon^2}{\mu_o} \sin^2 \theta \text{ N/m}^2 \quad (7)$$

which, with $B_\epsilon = 1.5 \text{ T}$, corresponds to a maximum pressure of $35.8 \times 10^5 \text{ N/m}^2$ at $\theta = \pm \pi/2$.

In the present application, the cylinder is composed of two half-shells, with their line of separation at $\theta = \pm \pi/2$. The geometrical symmetry of the cylinder requires that the currents induced in the shells obey the condition

$$\int_{-\pi/2}^{\pi/2} j_z d\theta = 0 \quad (8)$$

Then if the dividing plane between the two half-cylinders is rotated about the

longitudinal axis through a small angle δ with respect to the applied field, we speculate that this rotation will result in an interior field of magnitude $B_c \sin \delta$, in a direction normal to the slots. This field produces a torque on the tube, whose magnitude per unit length will depend, among others, on the slot width and on the radius of the shells. We have attempted to measure this torque but our method proved to be insufficiently sensitive to determine the functional relationship of the relevant variables unambiguously. The torque can be quite large: at 1.0 T and 10 degrees rotation, the largest value measured was about 50 Nm per meter length of shield.

Thus to shield an external field of 1.5 T, we require a superconductor with a minimum critical current density of about $2.5 \times 10^9 \text{ A m}^{-2}$, and a supporting structure designed to withstand a pressure of some 40 atmospheres, directed inwardly for flux exclusion but directed outwardly should flux become trapped inside. The structure must also resist the considerable torsional forces in addition to being capable of precise alignment. The gap between the two semi-cylinders of the superconductor must be small compared with the radius of the tube, in order to minimize field penetration.

3. Early Development Work

Our early attempts at constructing a flux-excluding tube were based on the assumptions that (a) niobium-titanium foil would have to be used, (b) adequate liquid helium permeation for cooling purposes is essential, and (c) the direction of the rolling of the foil is important, insofar as it produced a grain orientation which might enhance the critical current characteristics of the superconductor in a preferred direction.

We used various thicknesses of Nb-Ti foil, from 300 μm down to 33 μm , with and without interleaved copper spacers. The construction involved winding 30 cm wide material around a stainless steel mandrel into a multilayer spiral. Winding was either by hand, with little control over the tightness of the roll, or on a lathe with careful tension control. The samples were placed in a liquid helium bath and an external transverse magnetic field applied. The field inside and outside the shielding cylinders was continuously monitored. Typically, no field penetration would be observed below ~ 0.6 T. Above this applied field, a flux jump would occur, with either partial or full penetration of the external field. A further increase (or decrease) of the external field would result in no immediate change in the trapped internal field until the applied field had changed by more than about 5 percent, and then further flux jumps could be produced. We judged the quality of our shield tubes by the strength of the external field at the point where the first flux jump occurred. Usually the hand-wound samples produced mediocre shielding results and the tests often resulted in samples that were badly distorted by the magnetic forces. The machine-wound samples fared better: 10 effective turns would shield up to 0.65 T, as shown in Fig. 2. On the other hand, additional turns did not seem to improve the shielding characteristics proportionately. Reducing the temperature of the liquid helium to 2⁰ K did not significantly improve the shielding

characteristics. We concluded that adequate cooling did not appear to be limiting the shielding factor. Also, experiments not directly concerned with the shielding of magnetic fields suggested to us that the lack of mechanical stability, a feature common to all of our tests so far, might be preventing us from reaching greater shielding factors. In samples which were tested repeatedly, frequently with a trapped field remaining after the external field had been reduced to zero, we observed a progressive reduction in the shielding capability. Usually this reduction could be correlated with mechanical deformation of the shielding tube by the cumulative cyclic effect of the magnetic forces.

One further set of experiments should be mentioned here. It has been brought to our attention that the Linde Division of the Union Carbide Corporation had developed a process⁷ for making high-field superconducting alloys by plasma plating niobium and tin and other powder blends onto shaped carrier substrates, followed by an appropriate heat treatment of the composite. We acquired two tubular composites, one made of Nb₃Sn, the other of Nb_xTi. The behavior of the Nb₃Sn tube is shown in Fig. 3; the Nb_xTi tube failed to shield more than 0.1 T. Again the shielding was relatively unsatisfactory for reasons that we were unable to explain. As we saw no immediate improvement in the shielding characteristics and as we clearly had no control over the fabrication process, this method was considered to be unsuitable for our application. We therefore turned our attention to the remaining alternative, namely, Nb₃Sn tape.

As furnished by KBI,⁸ this material consists of a 6 - 12 μm thick niobium substrate carrying on both sides a 2 - 3 μm thick layer of Nb₃Sn which in turn is protected by a layer of electrolytic copper, the whole sandwich being about 30 to 35 μm thick. The critical current at 4.2°K and 10 T of 5-cm wide tape is about 150 A. In the first series of experiments, the foil tape was spirally wound under

constant tension on stainless steel mandrels 1 cm in diameter and 10 cm long. No additional copper strip was used and no attempt was made to provide extra cooling passages. The samples were prevented from unrolling by mechanical clamps. All measurements were made by mounting the tubes transversely at the center of a 15-cm bore superconducting solenoid, capable of providing a field of 1.2 ± 0.2 T over the tape. The samples prepared in this manner, besides their rather erratic shielding behavior, often exhibited considerable mechanical disturbance, even damage, at the end of the tests. This reinforced our earlier conclusions that mechanical distortion of the material was primarily responsible for the degradation in performance.

The same material used in the above tests was coated on both sides with a thin layer of Wood's alloy and warmed during the wrapping process. The end product, a rigid, monolithic, spiral roll of superconducting tape, was tested as before. Typically, a tube made up of 6 layers of superconductor (3 turns) would shield ~ 0.5 T after which the field would penetrate smoothly with no flux jumps. Figure 4 illustrates the improvement in performance which this technique effected. As the $90\text{-}\mu\text{m}$ thick tape proved rather difficult to work with, we switched to $120\text{-}\mu\text{m}$ material, which is a composite sandwich of two niobium tapes and four Nb_3Sn layers between two copper cladding layers, each $30\ \mu\text{m}$ thick. The critical current of a 5-cm wide strip at 4.2°K and 10 T is 300 A, or twice that of the thinner material. With this thicker and more manageable material, we were able to reproduce quite consistently the earlier results and our conclusions remained unchanged.

4. Laminated Semi-Cylinders

The spiral wrap technique, based on 5-cm wide modules, is obviously unsuitable for any kind of tubular construction involving long lengths. Quite apart

from edge effects which, as our measurements have shown, would have materially increased the number of layers per tesla required to shield the applied field, we found no solution to the problem of combining 5-cm wide tubes into an assembly some 4 m long. We therefore returned to the original concept of combining two semicircular shells into a long cylinder. The manufacturing process is illustrated in Fig. 5. First, an aluminum die in the form of a semi-cylinder was made, in which the requisite number of layers of superconductor were shaped. As Wood's alloy proved difficult to work with, we switched to a 60:40 eutectic lead-tin solder whose melting point of 184°C was still low enough not to affect the properties of the superconducting tape or to delaminate it. The aluminum die with the superconducting tape under compression was warmed to just above the melting point of the solder, additional solder being added as required. After the bonded material had cooled, the protruding superconductor and excess die material were milled off to produce two accurate semi-cylinders. The two completed semi-cylinders were placed around the copper-plated stainless steel mandrel and clamped between the two machined female sections of the original die. This assembly was reheated with the addition of solder as necessary to join the two semi-cylinders to the central tube. Depending on the type of measurement, additional clamping was provided by either modified hoseclamps or by sliding a heated tightly-fitting copper or stainless steel tubular sleeve over the superconductor. The irregular ends of the superconductor were usually machined off to provide samples of uniform length.

This method provided a consistent set of samples, the measurements of which will be described in the next section.

5. Experimental Measurements

With the exception of the initial experiments with NbTi foil tubes, which were studied in a C-magnet and in a large bending magnet, our measurements were made either transversely in the field of a 15-cm bore solenoid or in a split-coil superconducting magnet, with an iron yoke and shaped pole pieces, and a 5-cm gap.

The field internal to the tube was measured with a Hall plate; the applied field, initially calibrated using similar Hall plates, was obtained from the magnet energizing current. The performance of each sample tube was recorded both as an X-Y plot of the magnet current as a function of the internal Hall plate voltage, and as a digital record of the same data, plus the environmental parameters for the run. As our first series of measurements did not indicate a dependence of the shielding characteristics on the rate of change of the applied magnetic field (at least to within the accuracy of our measurements), no attempt was made to control the charging rate of the magnet. However, the characteristics of the magnet were such that rates in excess of 0.5 T per minute were achieved only in a very few measurements, and most measurements were made at rates of about 0.35 T per minute. A typical shielding curve ($B_{\text{ext}} = I_{\text{applied}}$ vs $B_{\text{int}} = V_{\text{Hall}}$) is shown in Fig. 6. The smoothness of the penetration of the field into the shielding tube and its reversibility proved to be, after we gained experience, a measure of the skill and care with which the sample was assembled. Towards the end of our program, we were able to predict the behavior of our samples from their manufacturing history: If the tube went together well, without rework, usually no discontinuous behavior was observed. If, on the other hand, the solder did not wet the superconductor properly, or if the final reheating cycle was inadequate, or if the solder became overheated, the sample would almost certainly display

discontinuous field penetration. In every case where the tube sample failed by a flux jump, we were able to restore the smooth field penetration characteristics by careful rework of the sample, either by resoldering or by providing additional mechanical supports or both. We were unable to detect any effects which could be ascribed to local instabilities caused by thermal gradients, overheating of the superconductor or local hot spots, using samples that were encased in stainless steel, copper, or were left bare. We also endeavored to examine the effect of increasing or decreasing the amount of copper in the superconductor as a function of the rate of change of the applied field. Doubling the copper content of our tapes and increasing the magnet charging rates from 0.05 to 0.5 T per minute produced no effect detectable by our measuring equipment. We therefore concluded that within the accuracy of our apparatus, our application, and our technique, both temperature and dynamic stability effects are not observed. By contrast, however, mechanical deficiencies in the construction of our sample tubes would invariably lead to abrupt field penetration, and this would occur in a remarkably consistent pattern. We observed no "training" in this phenomenon. A tube that permitted the outside field to penetrate at 1.85 T one day would do so again, within ± 0.05 T, one month later.

Figure 7 illustrates the general behavior of shielding tubes constructed of Nb_3Sn tape from the same manufacturer. It is a plot of the external field at which flux penetration begins as a function of the number of layers of superconductor. All points are actual measurements made on numerous samples of various lengths, diameters, and numbers of layers of superconductor, taken over a period of months. Each point represents a series of measurements which, because of the high degree of reproducibility, cannot be resolved individually on the graph.

The regularity of this graph is striking, particularly when one considers that a considerable fraction of the superconductor in each sample is in the metastable critical state. We know from other evidence that this state is highly unstable and that very small disturbances in the applied field or temperature fluctuations will trigger a local catastrophic penetration of flux which may drive that region into the normal state. Since the penetration of flux is a regenerative process, we would expect this process to propagate through the tube. Our experimental evidence, however, seems to indicate the opposite. At no time did we experience the difficulties described by Firth et al., provided the mechanical integrity of the tube was unimpaired. As Fig. 7 shows, measurements made under very different experimental conditions and with different techniques are reproducible to a remarkable degree, even to the extent that a smooth curve through our data also passes very close to the point at which Firth et al. observed smooth flux penetration in their tests.

For geometrical reasons connected with the experiment, the diameter of the flux excluding tube was required to change along the beam. As it proved impractical to make a conical shielding tube assembly, a stepped construction was adopted with long superconductor overlap regions at each change in diameter. We made numerous samples of different diameters that could be nested inside one another and determined, as before, the shielding characteristics of such a composite as a function of the length of the region of overlap. A typical series of measurements is shown in Fig. 8. The overlap decreases from top to bottom. On the basis of these and similar measurements, we concluded that once the overlap length between two concentric shielding tubes exceeds the diameter of the larger tube, the shielding characteristics of the outer tube are maintained, and there is no discontinuity in the shielding across the overlap, provided, of course, the shielding capacity of the smaller or inner tube is not exceeded. These findings, incidentally, are in

qualitative agreement with the earlier work of Haid et al. The above comments apply only to the gross behavior of the overlap region; some local disturbance of the fields must necessarily occur at the ends of the respective tubes in the region of the current turnaround. We have indeed observed small anomalous field penetration effects under the rather specific condition where the external field is about to begin penetrating one or the other shielding tube. As the design of the final shielding tube certainly did not call for such a critical condition, we postponed the investigation of this effect to a later date.

6. The 4-meter Tube and Cryostat Construction

Figure 9 presents an exploded view of the shielding tube, its cryostat and the liquid helium supply dewar. The relatively stringent requirements of the experiment produced a complex structure: Although the shielding tube proper is only ~ 4 m long, the cryostat vacuum jacket had to be extended through a series of spark chambers and counters to the liquid helium supply, so that the overall length of the system is about 7.3 m. Further, the angle subtended by the tube at the target was restricted to 20 mradians and the maximum outside diameter of the vacuum jacket to 9 cm. Finally, the entire assembly was to be located to within ± 2 mm and aligned to within ± 125 μ m in the horizontal and vertical directions in the magnet and spark chamber system.

The mandrel supporting the superconducting half-cylinders is a stainless steel tube, the outside diameter of which increases in three steps from 9.5 mm to 15.7 mm to 19.0 mm. The outside of the tube was plated with 75 μ m of copper to facilitate the soldering process.

The superconducting shells are made in the manner described before but on a much larger scale in a special furnace and under accurate temperature control. Our experience with the soldering process convinced us that the pre-tinning operation of the superconducting tape is of crucial importance and we therefore ordered the tape for the final shielding tube already tinned by the manufacturer. The dies appropriate to each mandrel diameter were made in pairs, one for each semi-cylinder. The final assembly of the tube was made in the same jig and using the same dies in which each individual semi-cylinder was made. The overlap regions were made at least 50 cm long, and where required, brass filler shells were used to smooth out the transitions in the mandrel dimensions separating the superconductor subassemblies. In the final reheating and soldering process, great care was taken to minimize the amount of solder used and to achieve a good bond.

The number of layers of superconductor in each pair of shells was chosen so as to give a minimum safety factor of 2 in the thickness, as judged from the data of Fig. 7. The number of layers in each section is given in Fig. 9.

Starting at the upstream beam window, the helium vessel has a cylindrical geometry with a diameter that increases stepwise from 16 to 36 mm. At the collimator (see Fig. 9), the helium container is formed of a square stainless steel tube, 2.7 m long and 38 mm on a side, placed on edge.

In order to align the shielding tube and to hold it against the almost unavoidable torque, as well as to provide additional mechanical support, 17 octagonal

stainless steel spacers, 10 mm wide and 27 mm i.d., were slipped onto the outside of the tube. A brass split ring held within the octagonal spacer by four screws completed the support. The support spacers were aligned accurately along one face and locked in place. This assembly was inserted into the square helium vessel which now held the shielding tube rigid by virtue of its stiffness and resistance to torsion. After the helium fill line was inserted, the front cylindrical portion of the helium container was attached by welding to the square tube and by soft-soldering the inside mandrel to a copper-plated stub at the upstream end of the container. The downstream end of the helium container was capped by a stainless steel transition piece carrying the liquid fill and gas vent lines, the central beam tube, and a small instrumentation line.

The square portion of the helium vessel is held inside the vacuum tank on two low-conductivity supports which serve both to maintain the tube concentric with the vacuum tank and to transmit any torque forces to the suspension system. These two supports consist of perforated thin-wall stainless steel tubing, 50 cm long, their ends holding the square helium tank through two thin fiberglass spacers. The vacuum envelope has collars welded to it in two places, each collar having two threaded 6.5 mm diameter holes drilled through it. Two bolts per support pass through these holes to engage similar holes drilled in the perimeter of the central ring of each support tube. Standard 7-mm seal rings under each bolt head ensure the vacuum integrity of the system. Any torque experienced by the superconducting tube is therefore transmitted through the brass split rings to the octagonal spacers, to the square helium tank, to the support tubes and thence to the outside support system via the four bolts. The advantage of this system is that each component could be built and tested separately and the final misalignment error estimated from the tolerance stack-up.

At the upstream end of the system, where space limitations prevented this approach, no attempt was made to provide torque-resistant supports. The conical portion of the vacuum tank is a heavy-walled stainless steel spinning which slides into a collar on the cylindrical portion of the vacuum tank. An O-ring ensures vacuum integrity and a double row of lock screws engage corresponding V-grooves on the cone to facilitate alignment of the cone with respect to the cylinder. The apex of the cone has a short length of tube soldered to it, the inside flared end of which engages and centers the mandrel of the shielding tube. A second support, about one meter from the upstream end, supports the cylindrical portion of the helium tank. Since only the central portion of the helium tank is held, uniform shrinkage of the helium tank assembly on cool-down can take place from both ends.

At the downstream end of the helium vessel, simple fiberglass supports hold the beam tube, the supply, vent, and instrumentation tubes concentric with the vacuum tank. All components exposed to liquid helium temperature are electropolished and wrapped with an average of 60 layers of aluminized mylar superinsulation. The insulating vacuum is common to the beam tube, the main vacuum tank and to the liquid helium supply vessel. A blown 100 μm thick mylar window at the upstream end and a flat 350- μm mylar window at the downstream end complete the vacuum barriers.

The liquid helium supply vessel is a 30- ℓ capacity superinsulated cylindrical dewar with an intermediate helium vapor shield. The loss rate, when tested without the shielding tube, is about 0.7 ℓ of helium per hour. Liquid helium is drawn off from the bottom of the supply vessel and injected under the hydrostatic head pressure (on the average about 30 cm of liquid) at a point about 1 m away from the upstream end of the tube. The vapor returns along the top edge of the square tube to the exhaust vent. Under normal operating conditions, this vent is filled

with a two-phase mixture, the motion of which increases the driving force with which the liquid passes through the system. The system requires careful adjustment of the differential pressure between the fill and vent lines. Too high a pressure results in a high boil-off, too low a pressure tends to starve the first several centimeters of the helium tank of liquid. Because of lack of space, the insulation in that region is just barely adequate and this produces a preferential warming-up of the superconductor.

The temperature and hence the level of liquid in the helium vessel is monitored along its length, both inside and outside, by 270-ohm, nominal value, 1/8-watt Allen-Bradley calibrated carbon resistors. A 5-resistor ladder in the supply dewar activates the liquid level alarm and automatic fill system. To monitor the shielding performance, a Hall plate is mounted on an epoxy-fiberglass ring at the end of a long, 125 μm thick, mylar tube which reaches to the collimator when inserted into the vacuum space of the support mandrel from the upstream end. This arrangement makes replacement of the Hall plate possible in the event of its failure as the downstream end is not accessible, when the shielding tube is installed in the experimental set-up.

The shielding tube and its ancillary equipment were thoroughly tested before installation in the 54" magnet and the various loss rates measured. The boil-off is necessarily liquid level dependent: with a 40-cm liquid level in the supply dewar the boil-off averaged around 12 ℓ per hour, while with a liquid height of only 10 cm, the loss dropped to 7.5 ℓ per hour. Over a 24-hour period, the loss rate averaged about 10 ℓ per hour.

7. Results with Beam

The shielding tube was suspended in the magnet on 6 sets of 160 μm thick stainless steel cables pretensioned to \sim 300 pounds each with 20-cm steel

turnbuckles. The alignment procedure consisted of sequential adjustment of the turnbuckles while sighting optically through the bore of the tube before the final installation of the upstream beam window. An accuracy of ± 0.25 mm in the vertical and horizontal directions was thereby achieved. Before the first cool-down, the effect of the magnetic field on the warm tube was examined, and the internal Hall plate calibrated.

The cooldown of the tube takes on the average 7 hours from the time liquid is first admitted to the point where the temperature in the tube has stabilized. The average rate of supply of liquid over this period is about 16 liters per hour with about double that rate during the final filling operation.

The 54" magnet was initially energized to 1.05 T at the rate of approximately 0.1 T per minute in steps of ~ 0.3 T with a waiting period of some 30 minutes between each step. The Hall plate voltage changed from 1.195 mV to 1.220 mV, corresponding to a rise in the field inside the tube of 0.46 mT. An interesting phenomenon was observed at this point: The rate of change of the Hall plate voltage appeared to be time-dependent, as shown in Fig. 10 for external fields of 1.05, 1.25, and 1.5 T, which would indicate that a small fraction of the external field penetrated. The effect was very small: At 1.5 T, the maximum field recorded in the tube was 3.72 mT.

Beam studies with the shielding tube have provided us with some other results. The position and appearance of the beam spot were monitored at regular intervals by Polaroid photographs, a typical one of which is shown in Fig. 11 in which the appearance of the beam spot can be compared in the magnet-off and the magnet-on (1.5 T) situations. The peculiar displacement of the beam spot be explained by the superposition of two effects: one due to the fringe field of the magnet several meters up- and downstream of the shielding tube, the other due to a small remanent field component resulting from penetration effects. In the absence of the flux shield, the spot would be displaced vertically by ~ 200 mm.

The presence of the shielding tube in a uniform magnetic field produces some distortion of the local field which should be reflected in the field measurements. We have determined that the effect of the tube on the external magnetic field is a change of 0.1% in the field value as measured at the center of a pole piece.

To date, the tube and cryostat have been thermally cycled between room temperature and 4.2° K some sixteen times, including three physics runs, averaging twelve days each, spaced by inactive periods of some six weeks during which the system was warmed to ambient temperature, with no detectable degradation in performance. During the last run, the tube was maintained cold and superconducting for about fourteen days. On several occasions, malfunction of the magnet and its associated power supply system produced rapid variations in the magnetic field, resulting in penetration of a major fraction of the field into the tube. Each time this happened the tube was warmed up above the transition temperature in the presence of the magnetic field to minimize the effect of the magnetic stresses and the external field then reduced to zero. Upon cooldown and re-establishment of the operating conditions, it was found that the shielding properties of the tube remained unchanged and unaffected by the field penetration.

Acknowledgments

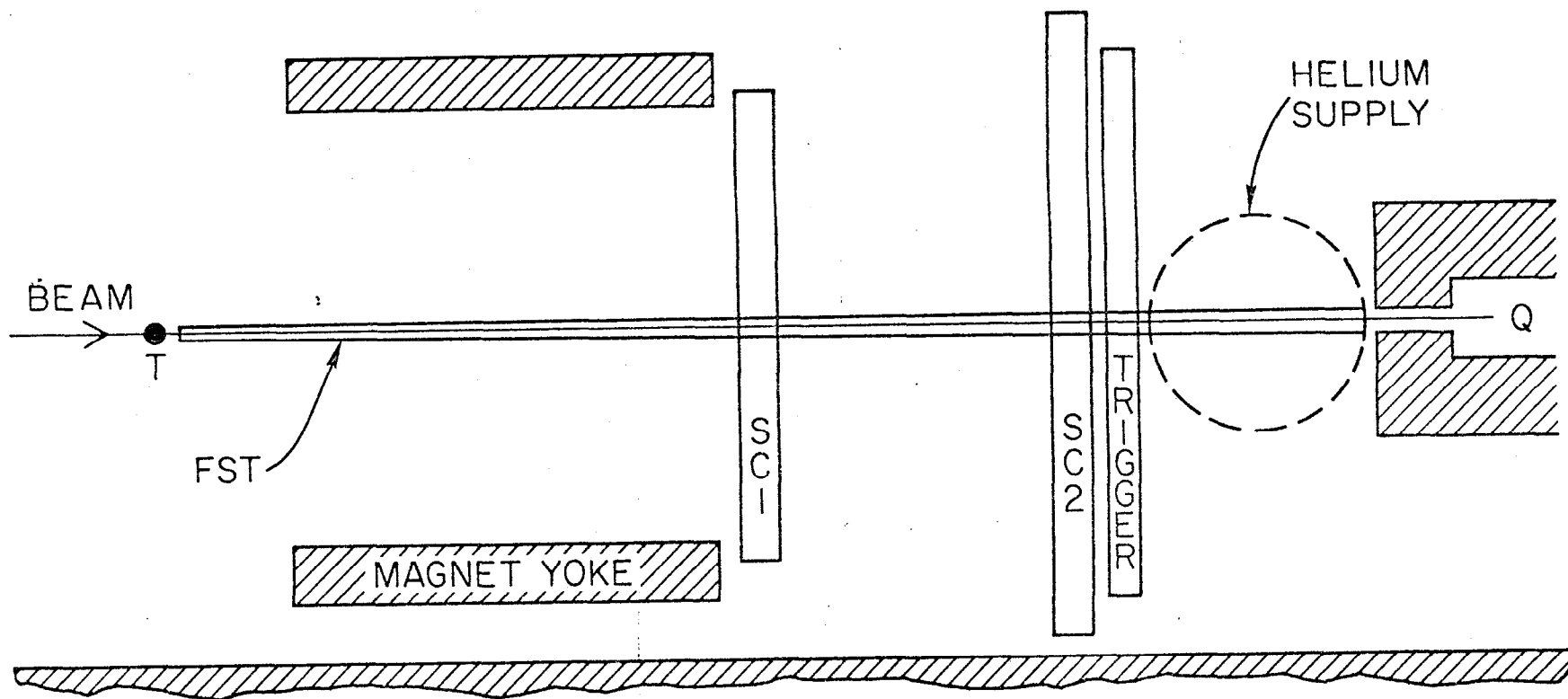
We wish to acknowledge our debt to Dr. M. Perl for his continued support and encouragement, and to Dr. H. Brechna for his assistance during the early phases of this work. Further, we should like to express our appreciation to our team of technical assistants, E. Gruenfeld, W. Kapica, A. C. Newton, E. Tillmann, and W. Wolff, without whom this project could hardly have been realized. We should also like to thank Mrs. V. Smoyer for help with that last and most important step, namely, the preparation of this manuscript.

References

1. B. Dieterle, W. Lakin, F. Martin, E. Petraske, M. L. Perl, J. Tenenbaum, and W. T. Toner, SLAC Proposal No. 65 (1970).
2. K. Heinloth, private communication.
3. J. C. Pratt, private communication.
4. M. Firth, L. Krempasky and F. Schmeissner, CERN TC-LTL Report (1969).
5. C. P. Bean, Phys. Rev. Letters 8, 250 (1962).
6. Y. B. Kim, C. F. Hempstead, and A. R. Strnad, Phys. Rev. Letters 9, 306 (1962).
7. D. A. Haid, C. A. Houck, C. R. McKinsey, Technical Report AFAPL-TR-67-155 (1968), Air Force Aero Propulsion Laboratory, Wright-Patterson Air Force Base, Ohio.
8. Kawecki Berylco Industries, P. O. Box 1462, Reading, Pa., U. S. distributors of Nb₃Sn tape manufactured by Thomson-CSF, 51 Boulevard de la République, 78, Chatou, France.

List of Figure Captions

- Fig. 1. General layout of experiment.
- Fig. 2. Flux penetration behavior of 300- μm NbTi spirally-wound foil tube.
- Fig. 3. Flux penetration behavior of a plasma-sprayed Nb_3Sn tube.
- Fig. 4. Flux penetration behavior of a Nb_3Sn spirally-wrapped foil, (a) layers mechanically clamped, (b) layers bonded by soldering with Wood's alloy.
- Fig. 5. The process for making shielding tubes from bonded semicircular shells.
- Fig. 6. Flux penetration behavior of a shielding tube made from two bonded semicircular shells.
- Fig. 7. Flux shielding characteristics of a number of tubes of various dimensions, as a function of the number of layers of superconductor.
- Fig. 8. Flux shielding characteristics of overlap regions.
- Fig. 9. Flux exclusion tube assembly in cryostat with liquid helium supply.
- Fig. 10. Hall plate voltage response as a function of time at 1.05, 1.25, and 1.5 T.
- Fig. 11. Appearance of beam spot without and with magnetic field.



BEAM: $e^{+(-)} 2 \times 10^4$ /pulse.

T: Liquid H_2/D_2 target. 4cms long.

FST: Superconducting flux shielding tube.

SC1, SC2: Optical spark chambers.

TRIGGER: Lead-lucite shower counters.

Q: Quantameter.

1 meter

1525A1

Fig. 1

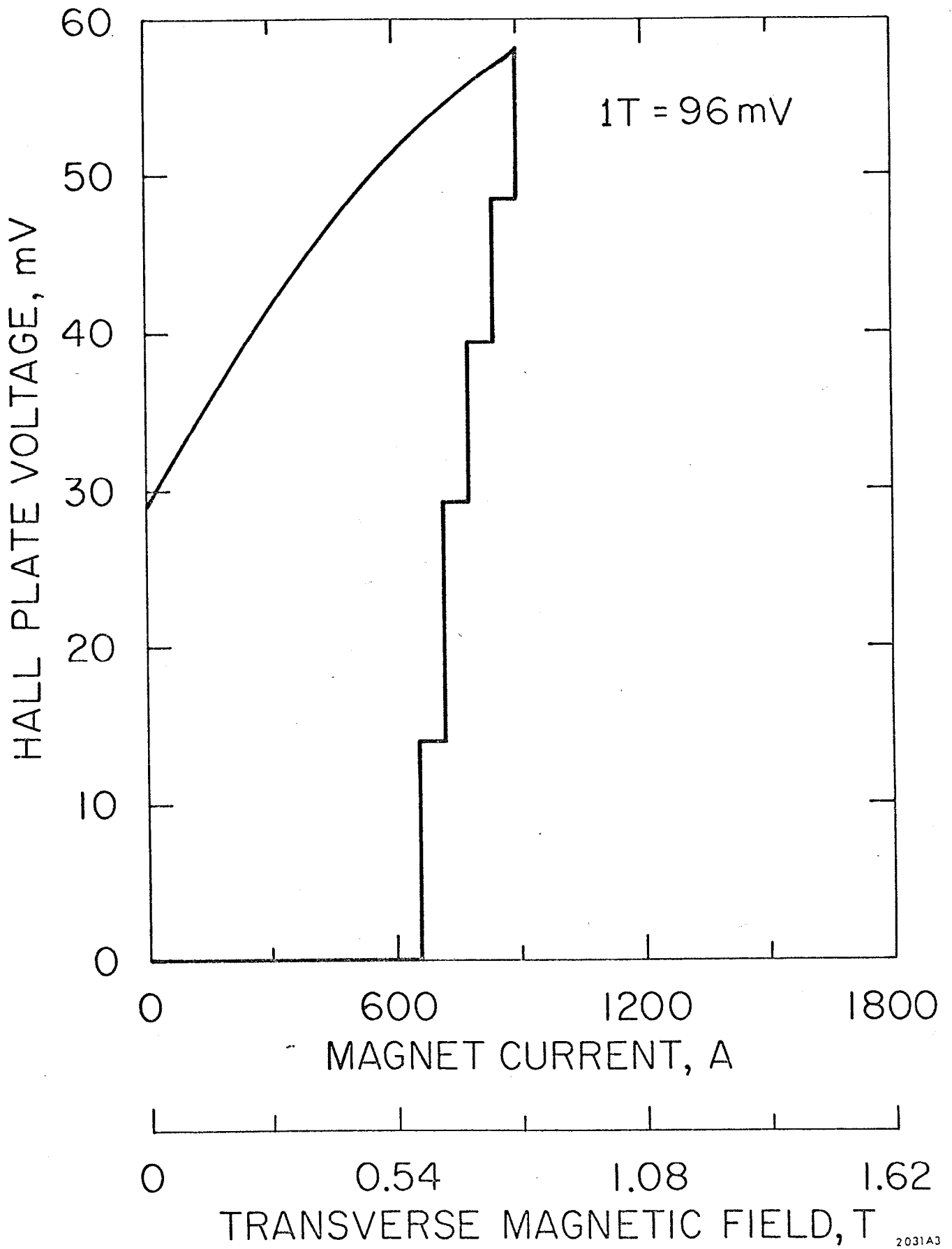


Fig. 2

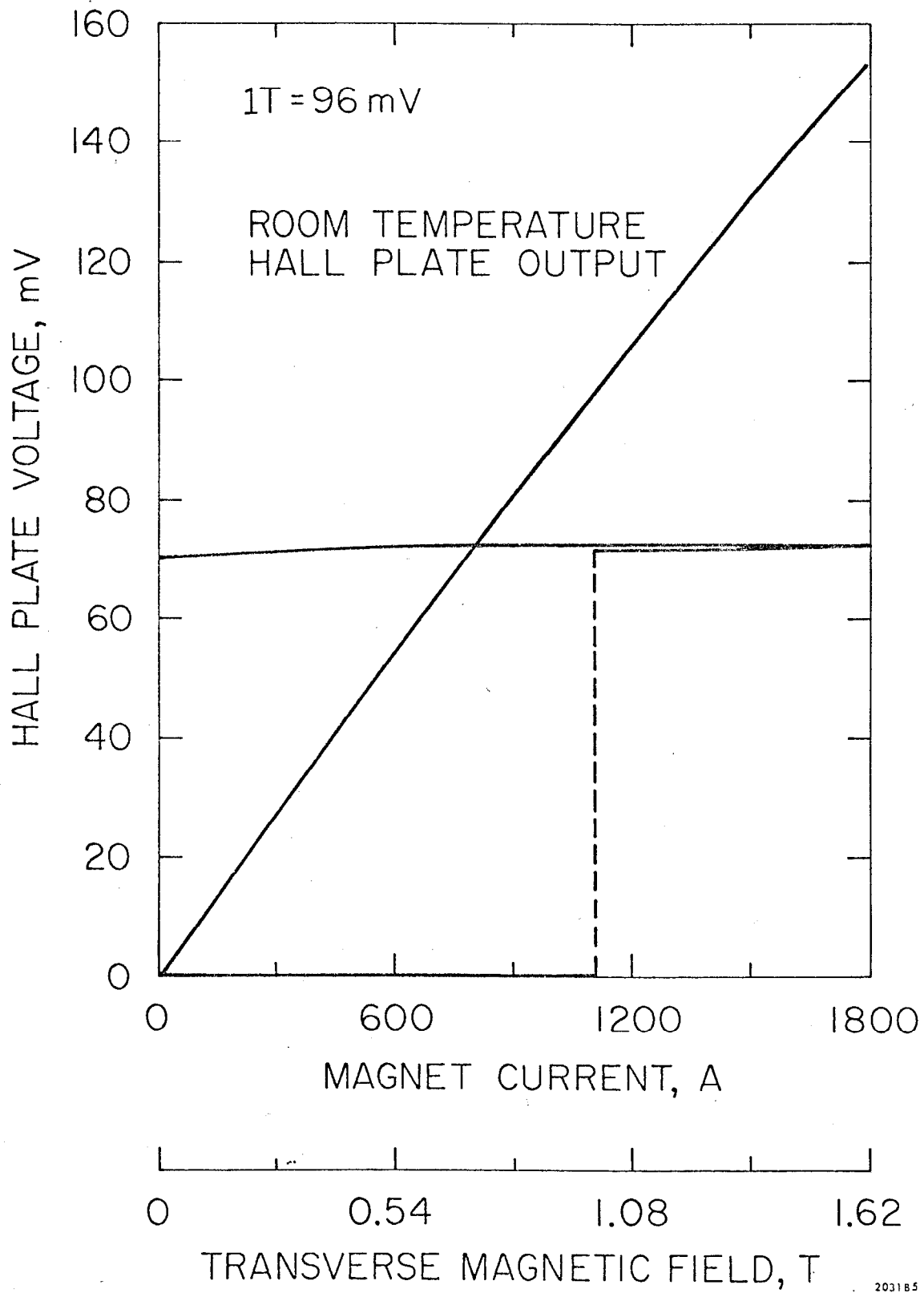


Fig. 3

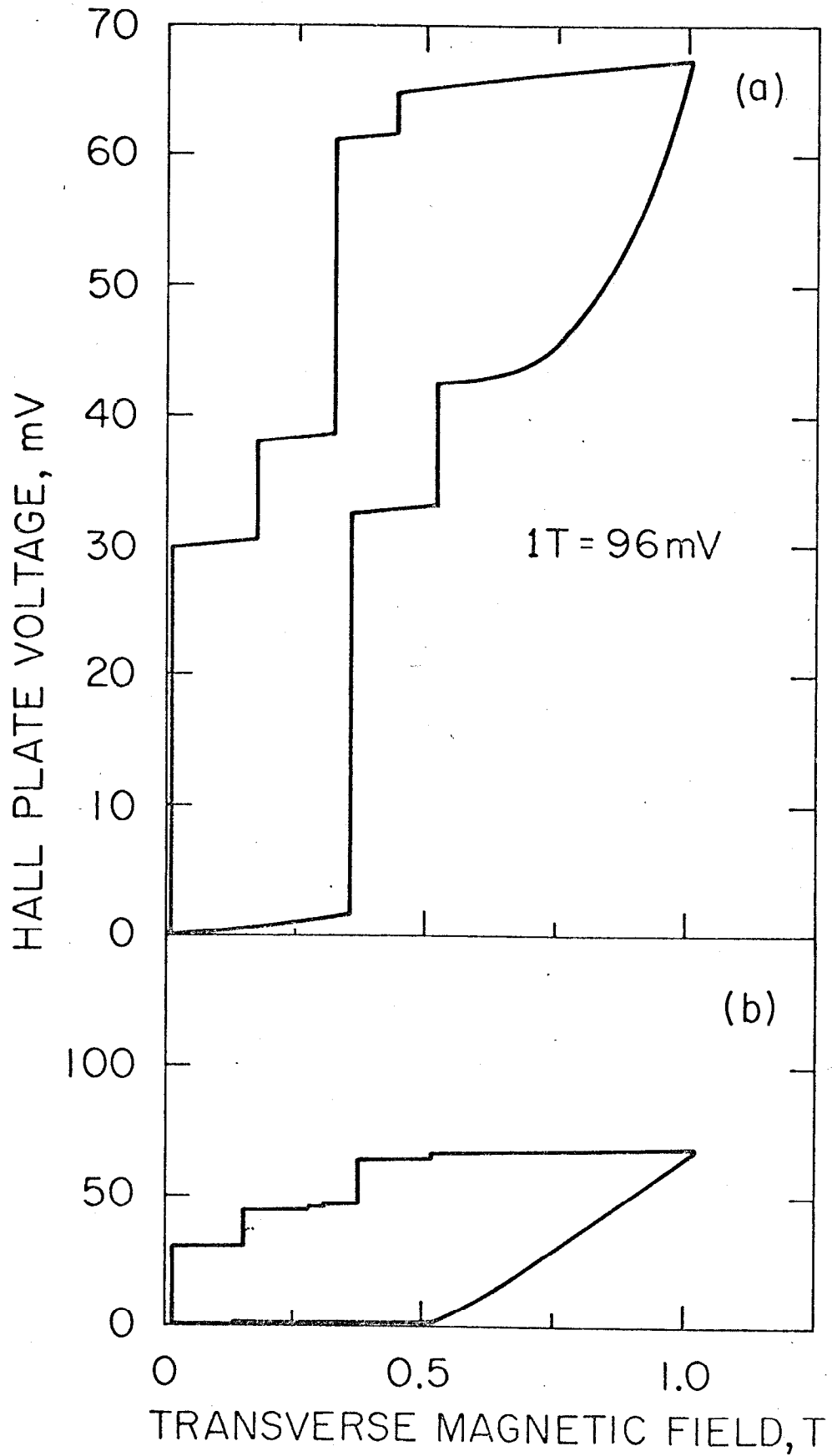
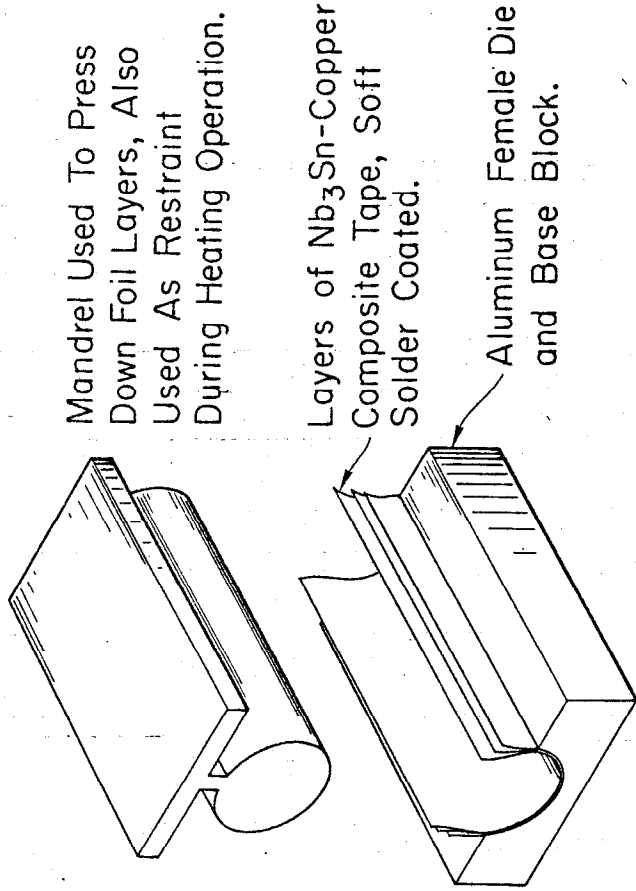
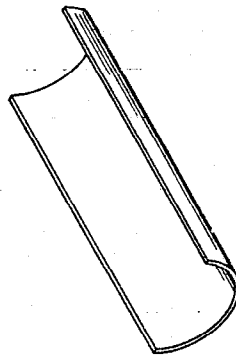


Fig. 4

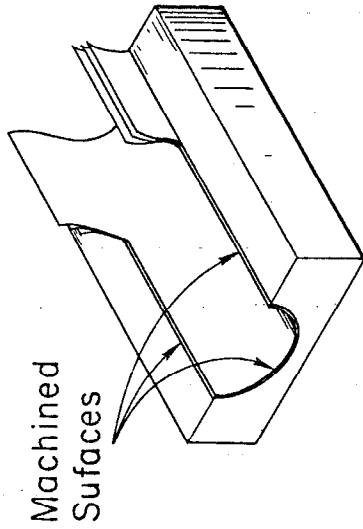
203186



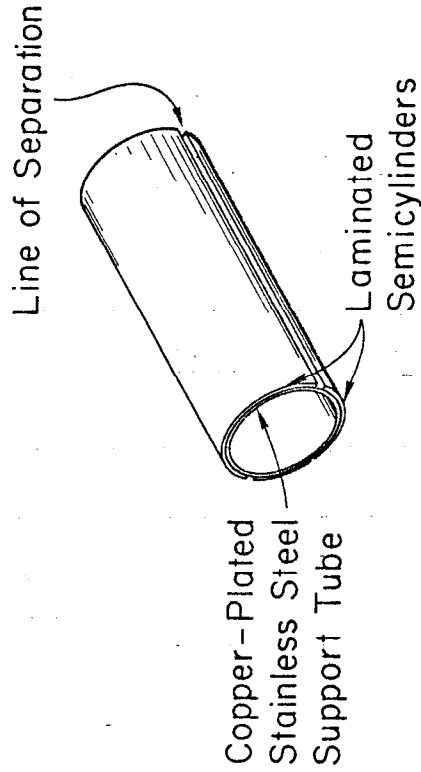
A. Lamination, Bonding with Solder and Shaping Operation.



C. Machined Semicylinder. Can Be Handled without Additional Support at This Stage.

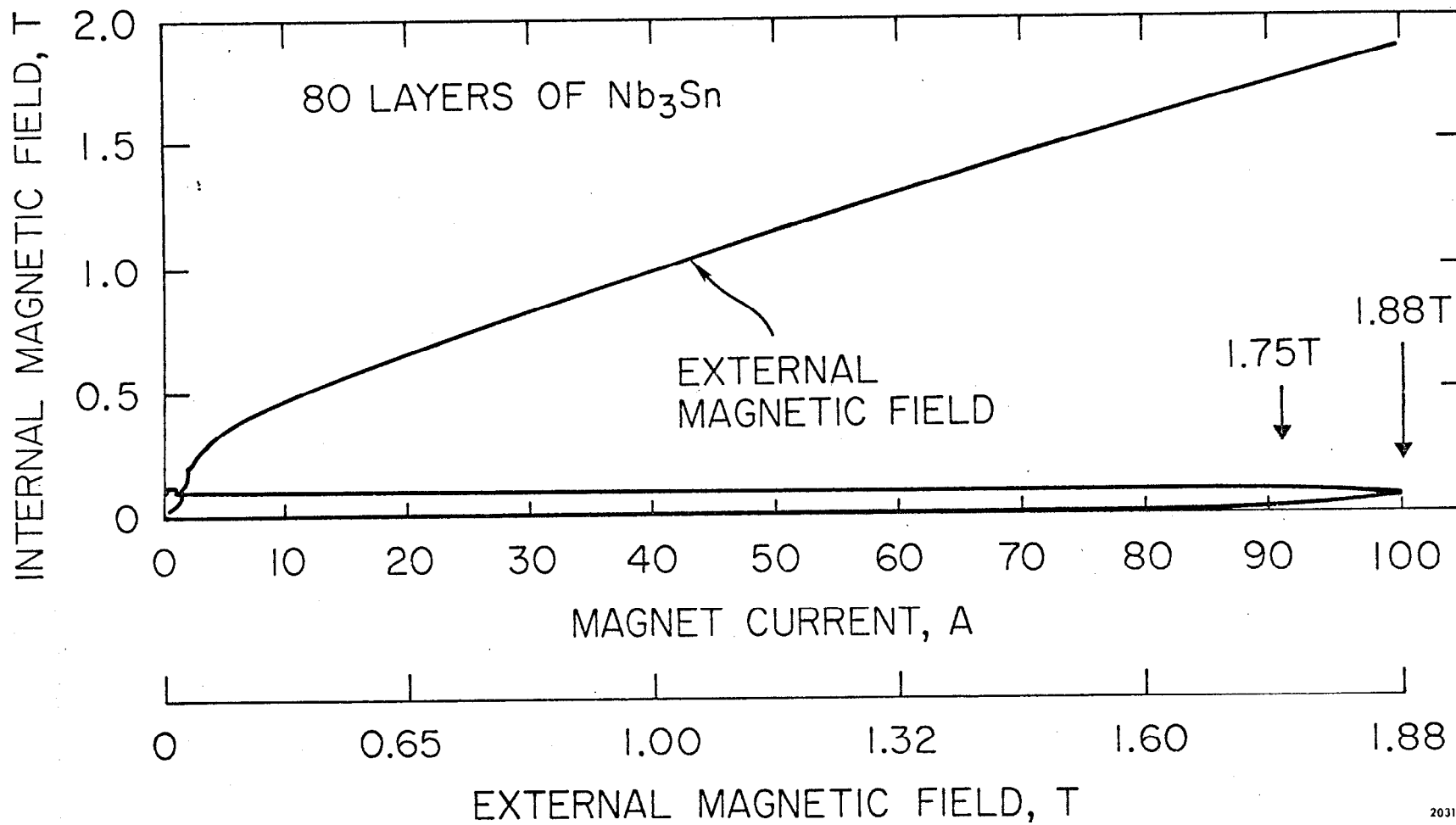


B. Machining Operation.



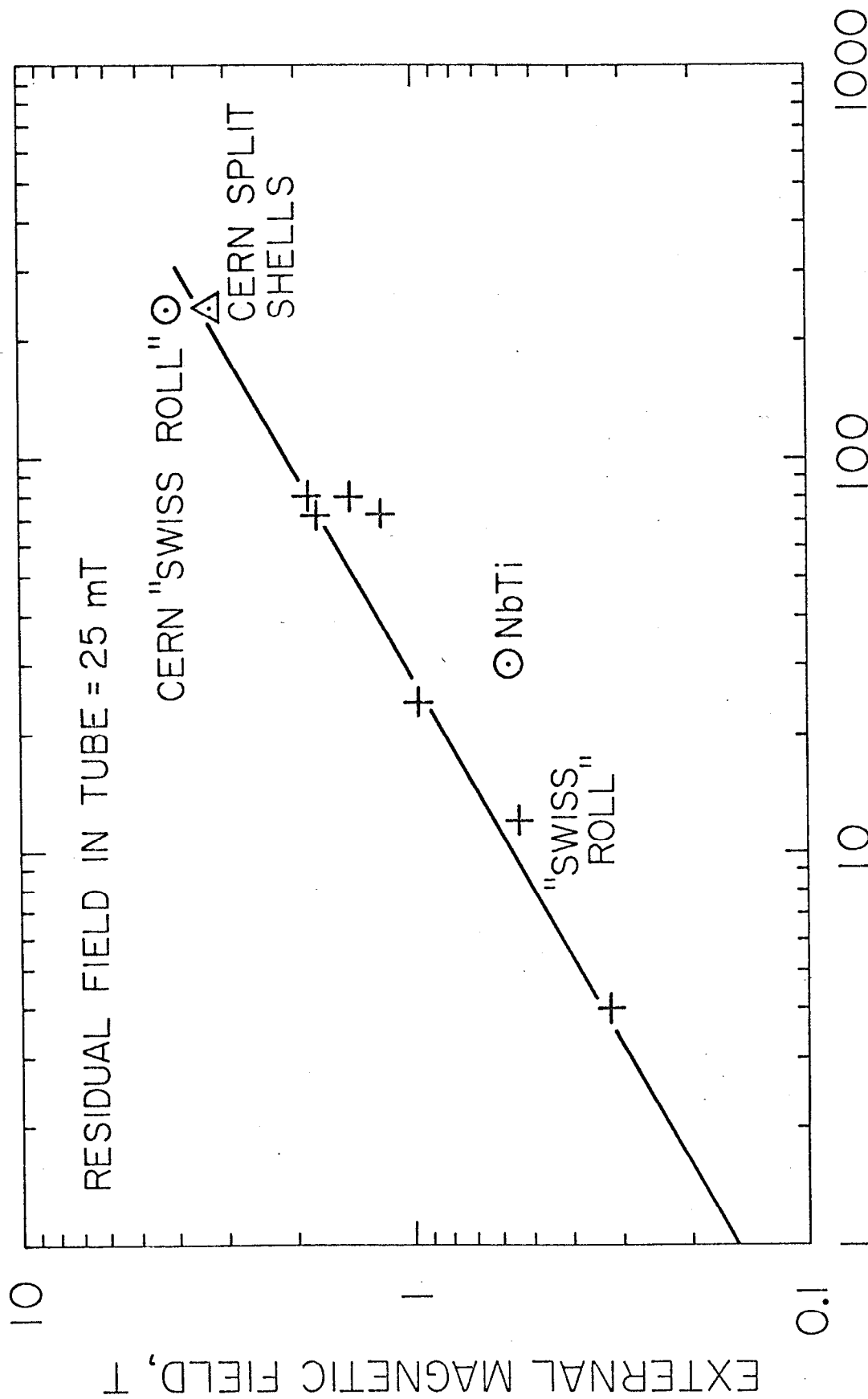
D. Finished Assembly, Bonded To The Stainless Steel Tube with Solder.

Fig. 5



203189

Fig. 6



NUMBER OF LAYERS OF Nb₃Sn

Fig. 7

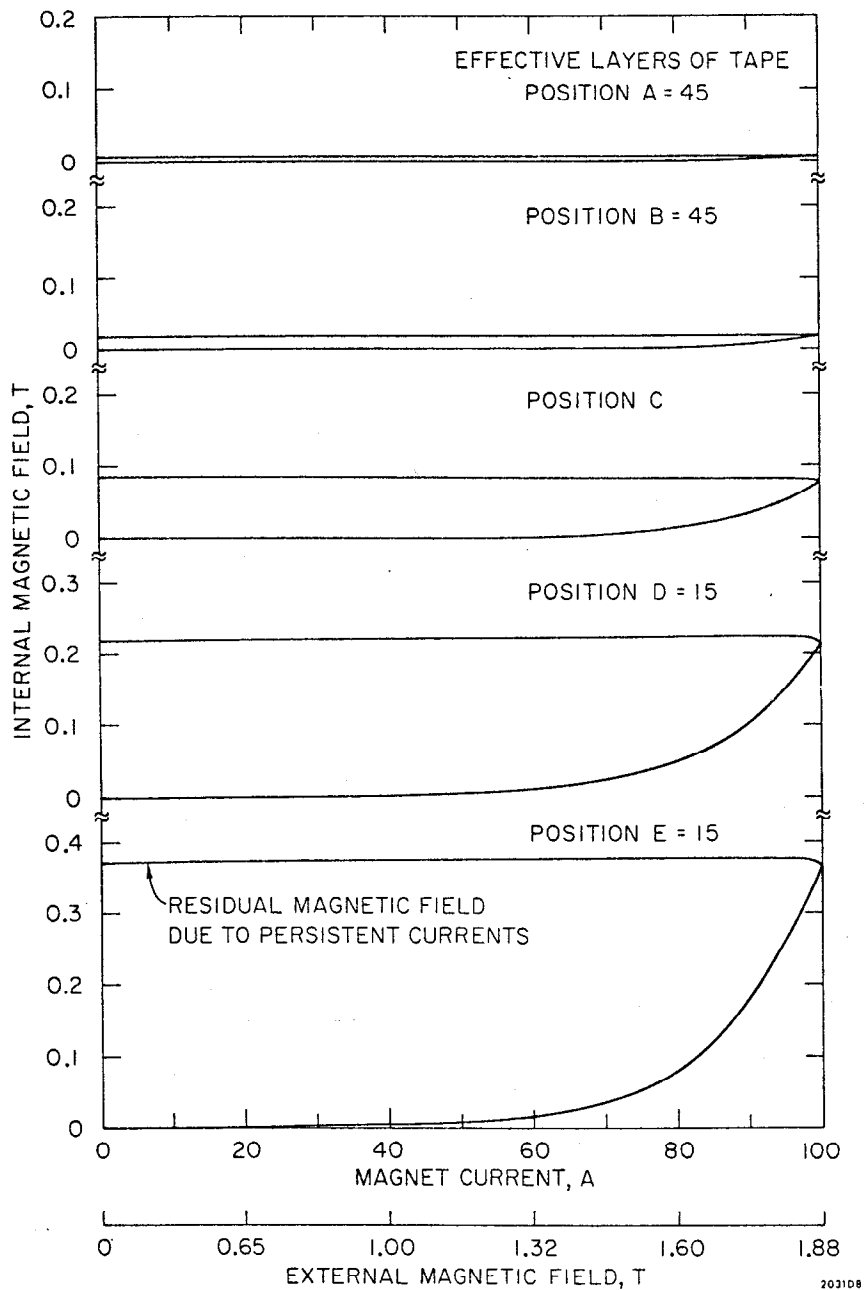
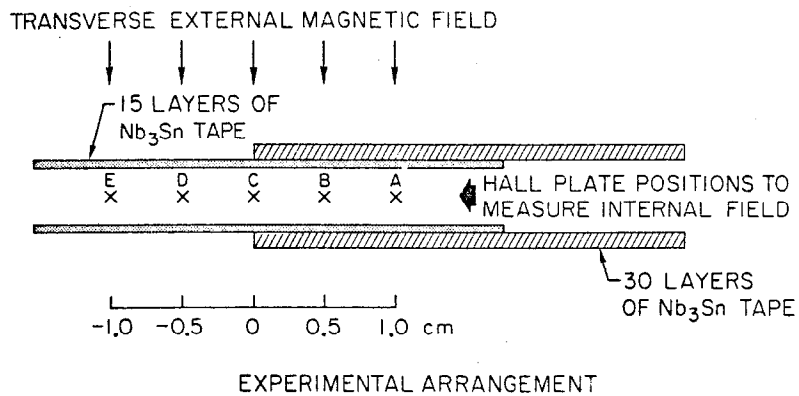
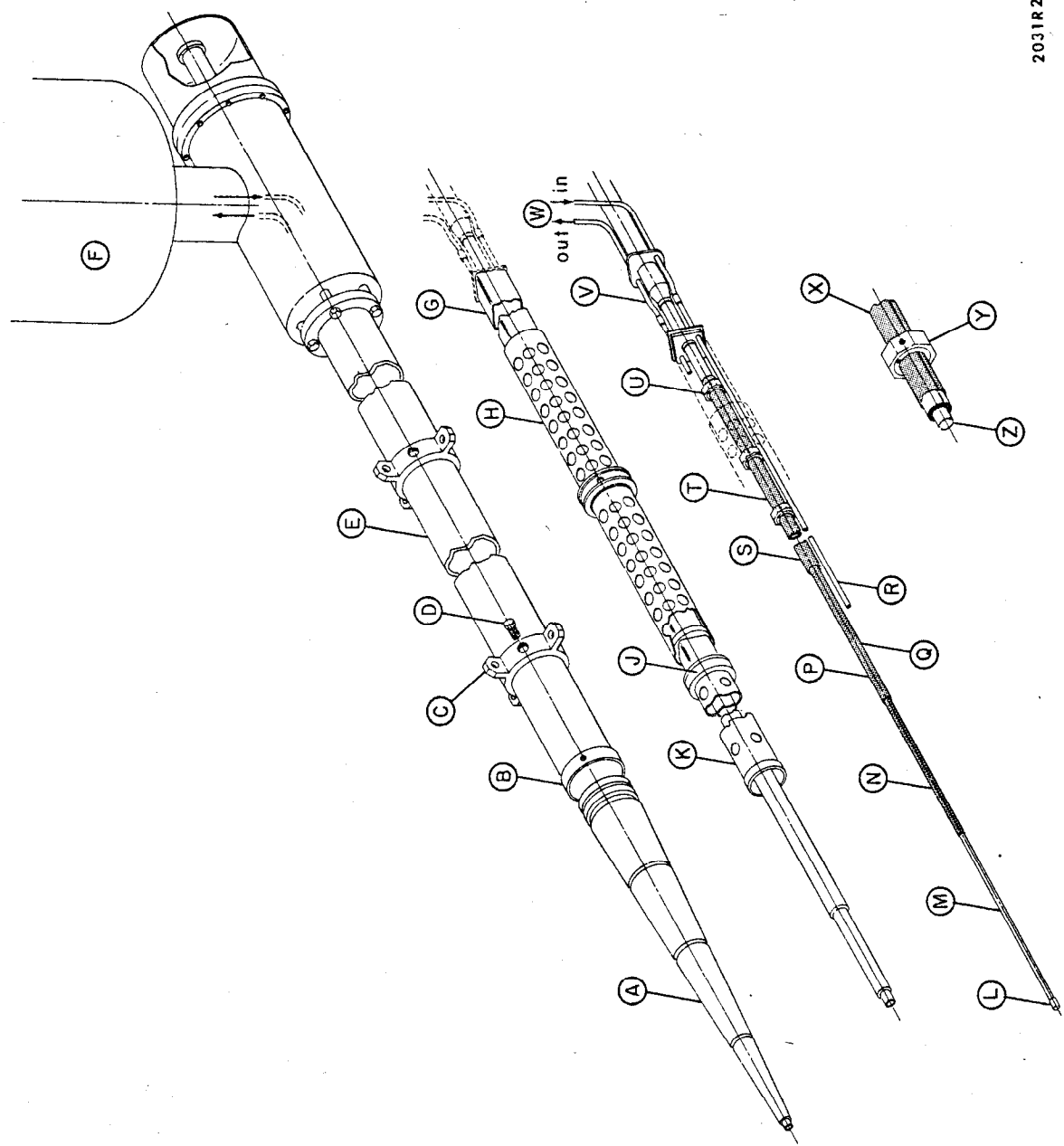


Fig. 8

7. 1/2 in. Diameter
Blunt Tip in Call
Tip of 1/2 in. Diameter



2031R2

Fig. 9

A Conical Vacuum Tank
B O-Ring Seal and Lockscrews
C Cable Support
D Locating Torque Bolt and
Vacuum Seal
E Cryostat Vacuum Jacket
F Liquid Helium Supply Dewar
and Instrumentation
G Square Helium Container
H Low Conductivity Torque Tube
Assembly
J Location of Collimator
K Cylindrical Helium Container
Support
L Mylar Beam Window
M Evacuated Beam Pipe
N 5 Layers of Superconductor
P Superconductor Assembly
Q 15 Layers of Superconductor
R Helium Fill Line
S Location of Brass Filler Shell
T 30 Layers of Superconductor
U Octagonal Support Spacers
V Helium Liquid and Vapor Return
Line
W Helium Supply and Instrumentation
Y Octagonal Stainless Steel Spacers
with Brass Split Rings, detail
Z Copper-Plated Stainless Steel
Mandrel

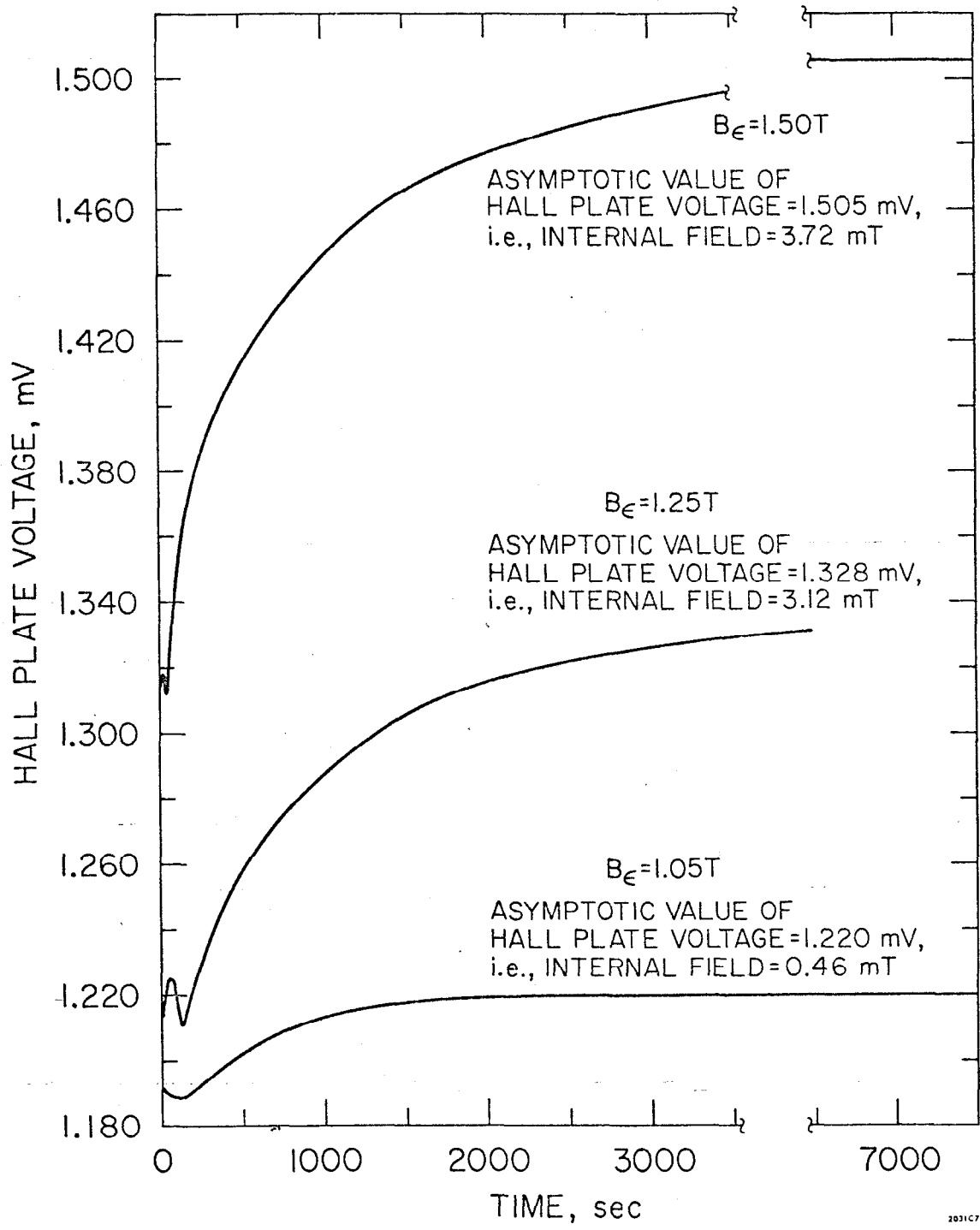


Fig. 10